

Extraordinary temperature dependence of the resonant Andreev reflection

Yu Zhu, Qing-feng Sun, and Tsung-han Lin*

State Key Laboratory for Mesoscopic Physics and Department of Physics, Peking University, Beijing 100871, China

(Received 27 April 2001; revised manuscript received 2 March 2001; published 12 September 2001)

An extraordinary temperature dependence of the resonant Andreev reflection via discrete energy level in a normal-metal/quantum-dot/superconductor (N -QD- S) system is predicted theoretically by using Green-function technique. The width of zero-bias conductance peak in N -QD- S is about $\sqrt{\Gamma_L^2 + \Gamma_R^2}$ and does not exhibit thermal broadening, where Γ_L and Γ_R are the coupling strength between QD and leads. Considering the intradot Coulomb interaction, the Coulomb blockade-oscillations conducted by Andreev reflection differs dramatically from that in N -QD- N . Instead of thermal broadening, finite-temperature induces more resonant peaks around the oscillation peaks of zero temperature. This effect can be applied to determine the coupling strength and QD level spacing in N -QD- S .

DOI: 10.1103/PhysRevB.64.134521

PACS number(s): 74.50.+r, 72.15.Nj, 73.40.Gk, 73.21.-b

Mesoscopic hybrid normal-metal/superconductor (N/S) systems have been investigated intensively in the last decade. Aside from their potential applications, these systems provide us an opportunity to combine with the two different quantum coherent behaviors, the coherence of quasiparticles in mesoscopic system and the coherence Cooper pairs in superconductors. The key mechanism to connect the above two together is the Andreev reflection (AR) process at the N/S interface.^{1,2} Many new phenomena and effects involving AR have been addressed in recent years (for a review see³ and references therein). Among them, normal metal/quantum dot/superconductor (N -QD- S) is one of the interesting systems, in which resonant AR occurs via discrete energy levels of QD.⁴⁻⁶ Considering the strong intradot interaction, the problem of Kondo resonance in N -QD- S were also studied by several authors.⁷⁻¹¹ In this paper, we shall predict the unique temperature dependence of the resonant AR process and investigate the interplay of Coulomb blockade effect and the Andreev tunneling in the N -QD- S systems.

Temperature usually gives the impression of averaging and smearing. At finite temperature, the sharp-resonant conductance peak usually has a thermal broadening of the order of $k_B T$, but we find this is not true for the case of resonant AR conductance. Let us begin by considering a N -QD- S system modeled by the following Hamiltonian,

$$H = H_L + H_R + H_{dot} + H_T,$$

$$H_L = \sum_{k\sigma} \epsilon_k a_{k\sigma}^\dagger a_{k\sigma},$$

$$H_R = \sum_{p\sigma} \epsilon_p b_{p\sigma}^\dagger b_{p\sigma} + \sum_p (\Delta b_{p\uparrow}^\dagger b_{-p\downarrow}^\dagger + \text{H.c.}), \quad (1)$$

$$H_{dot} = \sum_{\sigma} E_0 c_{\sigma}^\dagger c_{\sigma},$$

$$H_T = \sum_{k\sigma} (t_L a_{k\sigma}^\dagger c_{\sigma} + \text{H.c.}) + \sum_{p\sigma} (t_R b_{p\sigma}^\dagger c_{\sigma} + \text{H.c.}),$$

where H_L and H_R describe the left N lead and the right S lead, H_{dot} describes QD with one spin-degenerate energy level, and H_T is the tunneling between them.

In the regime of $k_B T \ll \Delta$, the zero-bias conductance is dominated by the AR process, and can be derived by using Green-function technique (see Ref. 6) as,

$$G_{NDS} = \frac{4e^2}{h} \int d\omega \left[-\frac{\partial f(\omega)}{\partial \omega} \right] \Gamma_L^2 |G_{12}^r(\omega)|^2, \quad (2)$$

where $f(\omega)$ is the Fermi distribution function, Γ_L is the coupling strength (defined later), G_{12}^r is the 12 element of 2×2 Nambu matrix \mathbf{G}^r , depicting the conversion from an electron into a hole. \mathbf{G}^r is defined by

$$\mathbf{G}^r(\omega) = \int dt e^{-i\omega t} (-i)\theta(t) \times \begin{pmatrix} \langle \{c_{\uparrow}(t), c_{\uparrow}^\dagger(0)\} \rangle & \langle \{c_{\uparrow}(t), c_{\downarrow}(0)\} \rangle \\ \langle \{c_{\downarrow}^\dagger(t), c_{\uparrow}^\dagger(0)\} \rangle & \langle \{c_{\downarrow}^\dagger(t), c_{\downarrow}(0)\} \rangle \end{pmatrix}, \quad (3)$$

and can be solved from the Dyson equation,

$$\mathbf{G}^r = \mathbf{g}^r + \mathbf{g}^r \boldsymbol{\Sigma}^r \mathbf{G}^r, \quad (4)$$

where

$$\mathbf{g}^r = \begin{pmatrix} \frac{1}{\omega - E_0 + i0^+} & 0 \\ 0 & \frac{1}{\omega + E_0 + i0^+} \end{pmatrix}, \quad (5)$$

$$\boldsymbol{\Sigma}^r = -\frac{i}{2}\Gamma_L \begin{pmatrix} 1 & 0 \\ 0 & 1 \end{pmatrix} - \frac{i}{2}\Gamma_R \rho_R \begin{pmatrix} 1 & -\frac{\Delta}{\omega} \\ -\frac{\Delta}{\omega} & 1 \end{pmatrix}, \quad (6)$$

in which

TABLE I. In the two limits of $k_B T \ll \Gamma_L, \Gamma_R$ and $k_B T \gg \Gamma_L, \Gamma_R$, the integrands of Eq. (2) and Eq. (8) can be evaluated, and the results are summarized here.

System	Condition	Conductance	Half peak width	Peak shape
N -QD- S	$k_B T \ll \Gamma_L, \Gamma_R$	$4(e^2/h)[\Gamma_L^2 \Gamma_R^2 / 4(E_0^2 + \Gamma_L^2 + \Gamma_R^2/4)^2]$	$0.64\sqrt{\Gamma_L^2 + \Gamma_R^2}$	Squared Lorentzian
N -QD- S	$k_B T \gg \Gamma_L, \Gamma_R$	$4(e^2/h)(\pi/4k_B T)\{\Gamma_L \Gamma_R^2 / 4(E_0^2 + [\Gamma_L^2 + \Gamma_R^2]/4)\}$	$\sqrt{\Gamma_L^2 + \Gamma_R^2}$	Lorentzian
N -QD- N	$k_B T \ll \Gamma_L, \Gamma_R$	$2(e^2/h)\{\Gamma_L \Gamma_R / E_0^2 + ([\Gamma_L + \Gamma_R]/2)^2\}$	$\Gamma_L + \Gamma_R$	Lorentzian
N -QD- N	$k_B T \gg \Gamma_L, \Gamma_R$	$2(e^2/h)(\pi/k_B T)[e^{\beta E_0} / (e^{\beta E_0} + 1)^2][2\Gamma_L \Gamma_R / (\Gamma_L + \Gamma_R)]$	$3.53k_B T$	Derivative of $f(\omega)$

$$\rho_R \equiv \begin{cases} \frac{|\omega|}{\sqrt{\omega^2 - \Delta^2}} & |\omega| > \Delta \\ \frac{\omega}{i\sqrt{\Delta^2 - \omega^2}} & |\omega| < \Delta \end{cases}, \quad (7)$$

and $\Gamma_{L/R} \equiv 2\pi N_{L/R} |t_{L/R}|^2$, with $N_{L/R}$ being the density of states in the left/right lead in normal state. For comparison we also write down the zero-bias conductance for N -QD- N ,¹²

$$G_{NDN} = \frac{2e^2}{h} \Gamma_L \Gamma_R \int d\omega \left[-\frac{\partial f(\omega)}{\partial \omega} \right] \frac{1}{(\omega - E_0)^2 + \left(\frac{\Gamma_L + \Gamma_R}{2} \right)^2}, \quad (8)$$

in which single-particle tunneling-process dominates. In deriving the above formulas, we assume that $\Gamma_{L/R}$ is independent of ω , which is reasonable in the calculation of zero-bias conductance.¹² In the two limits of $k_B T \ll \Gamma_L, \Gamma_R$ and $k_B T \gg \Gamma_L, \Gamma_R$, the integrands of Eq. (2) and Eq. (8) can be evaluated, and the results are summarized in Table I.

Figure 1 shows the curves of G_{NDS} vs E_0 and G_{NDN} vs E_0 at different temperatures for the symmetric coupling case $\Gamma_L = \Gamma_R \equiv \Gamma$. One can see the following features:

(1) For $T \rightarrow 0$, G_{NDS} has its maximum $4e^2/h$ at $E_0 = 0$ while G_{NDN} has $2e^2/h$, and G_{NDS} is much steeper than G_{NDN} , which is of the Lorentzian shape.

(2) With the increase of temperature, both G_{NDS} and G_{NDN} are suppressed, but surprisingly, the conductance peak of G_{NDS} does not exhibit thermal broadening while G_{NDN} obviously does.

Table I tells us that the peak width of G_{NDS} is always of the order $\sqrt{\Gamma_L^2 + \Gamma_R^2}$ for either $k_B T \ll \Gamma_L, \Gamma_R$ or $k_B T \gg \Gamma_L, \Gamma_R$. Feature (1) has been obtained in Ref. 4, while feature (2) is addressed for the first time in this work, to our knowledge.

Taking into account of that AR is a special two-particle process, feature (2) has a simple interpretation shown in Fig. 2. For N -QD- N [Fig. 2(b)], the conductance is dominated by the process of single-particle tunneling. At finite temperature, the Fermi surface of leads spreads out around the chemical potential in the range of $k_B T$, allowing incident electron has energy E in this range. The resonant tunneling occurs when $E_0 = E$, resulting in the broadening of conductance peak of the order $k_B T$. For N -QD- S [Fig. 2(a)], on the contrast, the single-particle tunneling is forbidden due to superconducting gap, and AR-process dominates. In the AR process, an inci-

dent electron with energy E (with respect to the superconductor chemical potential) picks up another electron with energy $-E$ to form Cooper pair and enter S , with a hole reflected in the Fermi sea of N . Since both the incident electron and the picked-electron pass QD through the discrete energy level E_0 , the resonant tunneling requires not only $E_0 = E$ but also $E_0 = -E$. Therefore, the resonant AR process occurs only when $E_0 = 0$, i.e., E_0 lines up with the chemical potential of superconductor. Because E_0 has a small broadening and shifting due to coupling with the leads, the condition $E_0 = 0$ becomes to $|E_0| < O(\Gamma)$ with $O(\Gamma)$ being the order of the coupling strength. Thus, the resonant AR causes a bottle neck of the conductance peak width in N -QD- S , leading to a broadening about Γ instead of $k_B T$.

Next, we investigate a more realistic model, in which QD has multiple single-particle energy levels and intradot Coulomb interaction, i.e.,

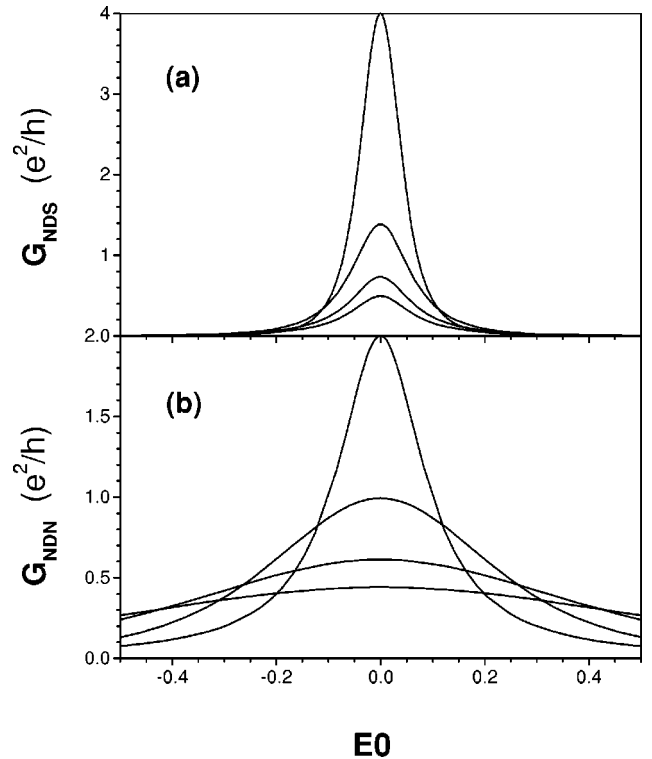


FIG. 1. The zero-bias conductance G vs the resonant level E_0 at different temperature for (a) N -QD- S and (b) N -QD- N . Parameters are: $\Gamma_L = \Gamma_R = 0.1$, $\Delta = 1$ for N -QD- S , $\Delta = 0$ for N -QD- N , $k_B T = 0.001, 0.1, 0.2, 0.3$ corresponding to the decrease of peak heights.

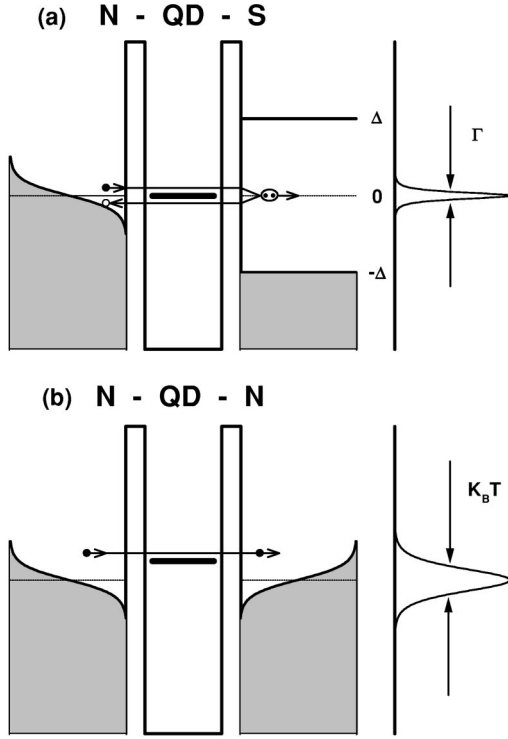


FIG. 2. Schematic picture for understanding the unusual temperature dependence of the conductance in Fig. 1. For (a) N -QD- S , resonant AR requires E_0 lines up with the chemical potential of the superconducting lead. For (b) N -QD- N , single-particle tunneling occurs when the resonant level E_0 within the range of $k_B T$.

$$H_{dot} = \sum_{i\sigma} E_i c_{i\sigma}^\dagger c_{i\sigma} + \frac{U}{2} \sum_{i\alpha \neq j\beta} n_{i\alpha} n_{j\beta}, \quad (9)$$

where i, j are indices of the single-particle energy levels, σ, α, β are indices of the spin, and U is the strength of Coulomb interaction. For N -QD- N with intradot Coulomb interaction, it is well known that the zero-bias conductance vs the gate voltage exhibits Coulomb blockade oscillations (CBO).¹⁴ For N -QD- S in which one of N electrodes is replaced by S , we also expect to see CBO except the conducting mechanism is AR. Taking into account of the unusual temperature dependence of the resonant AR process, CBO in N -QD- S may have significant change from that in N -QD- N .

We constrain ourselves to discuss the weak-coupling and low-temperature regime, i.e., $\Gamma \ll k_B T \ll \Delta$. If the coupling between QD and leads is weak enough, the atomic-limit solution¹³ ($\Gamma \rightarrow 0$) should be a good starting point. Because we study the zero-bias conductance, i.e., $V_L - V_R = 0^+$, QD can be viewed as in equilibrium, and the current driven by the small-bias voltage serves as a probe to the state of interacting QD. By generalizing the exact solution of the retarded Green function of QD in the atomic limit (see the Appendix for details), we propose the following scheme for the calculation of zero-bias conductance. Suppose QD has l spin-degenerate energy levels, $E_{1\uparrow}, E_{1\downarrow}, E_{2\uparrow}, E_{2\downarrow}, \dots, E_{l\uparrow}, E_{l\downarrow}$, with 2^{2l} configurations of occupation represented by $F = (N_{1\uparrow}, N_{1\downarrow}, N_{2\uparrow}, N_{2\downarrow}, \dots, N_{l\uparrow}, N_{l\downarrow})$ in which $N_{i\sigma} = 0$ or 1.

In the weak-coupling regime, the retarded Green function of QD can be derived by an approximated Dyson equation

$$\mathbf{G}^r = \tilde{\mathbf{g}}^r + \tilde{\mathbf{g}}^r \Sigma^r \mathbf{G}^r, \quad (10)$$

in which $\tilde{\mathbf{g}}^r$ is the atomic-limit solution for an isolated interacting QD and Σ^r is the self-energy caused by the tunneling between QD and leads. Σ^r is presented in Eq. (6), and $\tilde{\mathbf{g}}^r$ can be obtained as

$$\tilde{\mathbf{g}}^r \equiv \sum_F P(F) \mathbf{g}^r(F),$$

$$P(F) = \frac{1}{Z} e^{-\beta E_{dot}(F)}, \quad Z = \sum_F e^{-\beta E_{dot}(F)}, \quad (11)$$

$$\mathbf{g}^r(F) = \begin{pmatrix} \sum_i \frac{1}{\omega - \tilde{E}_{i\uparrow}(F) + i0^+} & 0 \\ 0 & \sum_i \frac{1}{\omega + \tilde{E}_{i\downarrow}(F) + i0^+} \end{pmatrix},$$

in which $E_{dot}(F) \equiv \sum_{i\sigma} E_{i\sigma} N_{i\sigma} + (U/2) \sum_{i\alpha \neq j\beta} N_{i\alpha} N_{j\beta}$ is the total energy of QD for the configuration F , and $\tilde{E}_{i\sigma}(F) \equiv E_{i\sigma} + U \sum_{j\beta \neq i\sigma} N_{j\beta}$ is the renormalized single-particle levels of QD. And the total conductance through QD can be expressed in terms of \mathbf{G}^r derived from the above equations.⁶

We plot G_{NDS} vs V_g and G_{NDN} vs V_g for different temperatures in Fig. 3(a)–3(d) and Fig. 3(e), where QD contains two spin-degenerate levels, $E_{1\uparrow} = E_{1\downarrow} = E_1 = V_g$, $E_{2\uparrow} = E_{2\downarrow} = E_2 = V_g + \Delta E$, with level spacing $\Delta E = 0.1$, interacting constant $U = 1$. For $k_B T \ll \Delta E$, we see typical CBO pattern in Fig. 3(a), with nearly equal-spaced peaks at $V_g = 0.0, 1.0, 2.1, 3.1$. With the increase of temperature, peak heights are suppressed, roughly proportional to $1/(k_B T)$ [Notice different scaling in Fig. 3(a)–(d)]. The most striking feature of CBO in N -QD- S is, when $k_B T \sim \Delta E$, temperature induces more resonant peaks around the original CBO peaks, instead of thermal broadening. One can see in Fig. 3(a)–(d) that the separation among peak groups is about U , while the spacing of peaks within one peak group is $\Delta E/2$, and each resonant peak has a width about Γ . Notice that all these properties are independent on temperature.

Qualitatively, this unusual pattern can be understood as follows. Due to the intradot Coulomb interaction, the original two resonances $E_1 = E_{1\uparrow} = E_{1\downarrow}$ and $E_2 = E_{2\uparrow} = E_{2\downarrow}$ exhibits eight subresonances, $E_1, E_2, E_1 + U, E_2 + U, E_1 + 2U, E_2 + 2U, E_1 + 3U, E_2 + 3U$ (see Appendix and Ref. 15 for detail). At zero temperature, only four resonances $E_1, E_1 + U, E_2 + 2U, E_2 + 3U$ are active, and the other four are Coulomb blocked. But for higher temperature of $k_B T \sim \Delta E$, the Coulomb blockade effect is partially removed. Not only E_1 but also E_2 are active and contribute to the total conductance. For N -QD- N , since resonant peak is broadened by finite temperature, the contributions of E_1 and E_2 are indistinguishable and combined to form the first CBO peak around $V_g = 0$ in Fig. 3(e). (This mechanism was first pro-

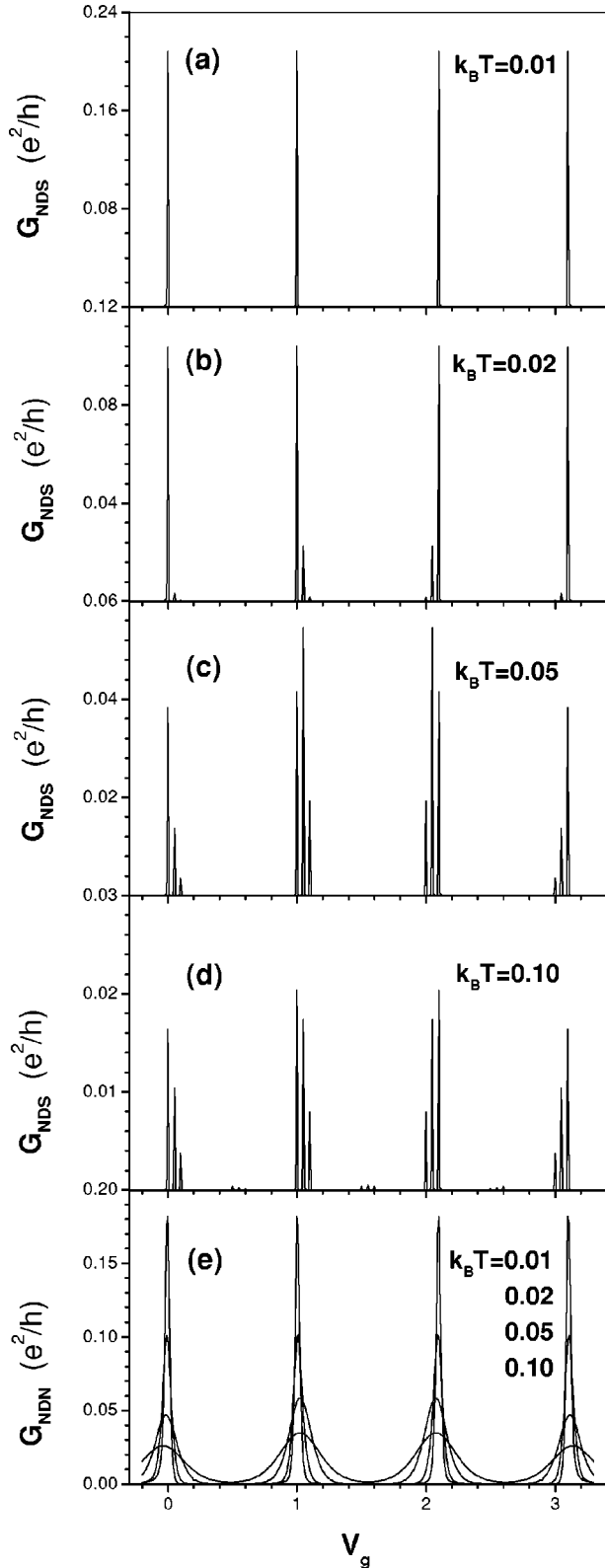


FIG. 3. Coulomb blockade oscillations of G vs V_g at different temperatures for N -QD- S in Fig. 3(a)–(d) and N -QD- N in (e). QD has two-spin degenerate levels, $E_{1\uparrow} = E_{1\downarrow} = E_1 = V_g$ and $E_{2\uparrow} = E_{2\downarrow} = E_2 = V_g + \Delta E$, with level spacing $\Delta E = 0.1$, Coulomb interacting strength $U = 1$. Other parameters are: $\Gamma \equiv \Gamma_1 = \Gamma_2 = 0.002$, $\Delta = 1$ for N -QD- S , $\Delta = 0$ for N -QD- N , $k_B T = 0.01, 0.02, 0.05, 0.10$ marked in the plots.

posed by Y. Meir *et al.* to explain the anomalous temperature dependence of CBO peak heights in N -QD- N .¹⁵ For N -QD- S , however, resonant AR peak has the width of Γ instead of $k_B T$. The first group of peaks around $V_g = 0$ in Fig. 3(c) consists of three distinguishable contributions of AR: AR via E_1 , AR via E_2 , and AR between E_1 and E_2 .⁶ Other groups of peaks can be understood similarly. Furthermore, one finds groups with tiny peaks around $V_g = 0.5, 1.5, 2.5$ in Fig. 3(d), which can be attributed to the AR process between E_1 and $E_1 + U$, E_1 and $E_2 + U$, E_2 and $E_2 + U$, E_2 and $E_1 + U$, etc. In short, temperature dependence of CBO in N -QD- S differs dramatically from that in N -QD- N .

Finally, we would like to make three remarks:

(1) The extraordinary temperature dependence of CBO in N -QD- S provides a new approach to determine the coupling strength $\Gamma \sim \sqrt{\Gamma_L^2 + \Gamma_R^2}$ and QD level spacing ΔE , which are impossible to do in N -QD- N because of thermal broadening.

(2) The suggested N -QD- S structure is accessible of the up-date nanotechnology, either by a metal nanoparticle connected to superconducting and normal-metal electrodes,^{16,17} or in a gate controlled N -2DEG- S structure.^{18–20} The key point to observe the predicted unusual temperature dependence of AR is to perform resonant AR process via discrete energy levels.

(3) Similar extraordinary temperature dependence of zero-bias conductance have been observed experimentally either in normal-metal/semiconductor/superconductor junctions²¹ or in normal-metal / high- T_c superconductor contacts.²² Perhaps, the discrete electronic state in our model corresponds to the quantum-well state and surface-bound state in their situations.

In conclusion, we predict an extraordinary temperature dependence of the resonant AR process in N -QD- S , in which the conductance peak does not exhibit thermal broadening. We also investigate CBO in N -QD- S , and find that finite-temperature induces more resonant peaks around the original CBO peaks of zero temperature, rather than gives them thermal broadening, which can be applied to determine Γ and ΔE in N -QD- S .

ACKNOWLEDGMENTS

This project was supported by NSFC under Grant No. 10074001. T.H.L. would also like to thank the support from the Visiting Scholar Foundation of State Key Laboratory for Mesoscopic Physics in Peking University.

APPENDIX

In this Appendix, we present the atomic solution in equilibrium, which is generalized to the weak-coupling case and linear-response regime in Sec. II.

In the atomic limit, QD is nearly isolated from the leads, and the negligible coupling to leads determines the equilibrium / nonequilibrium distribution in QD. Suppose QD has multiple discrete energy levels, indexed by $i = 1, 2, \dots, L$ (here i contains the spin index), and QD in the atomic limit can be described by

TABLE II. For the three-level QD, the results for the calculation of the correlation functions like $\langle n_1 n_2 \rangle$ are listed in the following table.

$\langle n_1 n_2 n_3 \rangle$	$(1/Z)e^{-\beta(E_1+E_2+E_3+3U)}$	$\langle n_1(1-n_2)(1-n_3) \rangle$	$(1/Z)e^{-\beta E_1}$
$\langle (1-n_1)n_2 n_3 \rangle$	$(1/Z)e^{-\beta(E_2+E_3+U)}$	$\langle (1-n_1)n_2(1-n_3) \rangle$	$(1/Z)e^{-\beta E_2}$
$\langle n_1(1-n_2)n_3 \rangle$	$(1/Z)e^{-\beta(E_1+E_3+U)}$	$\langle (1-n_1)(1-n_2)n_3 \rangle$	$(1/Z)e^{-\beta E_3}$
$\langle n_1 n_2(1-n_3) \rangle$	$(1/Z)e^{-\beta(E_1+E_2+U)}$	$\langle (1-n_1)(1-n_2)(1-n_3) \rangle$	$(1/Z)e^{-\beta \cdot 0}$

$$H_{dot} = \sum_{i=1}^L E_i c_i^\dagger c_i + U \sum_{i<j} n_i n_j, \quad (\text{A1})$$

in which the second term is the intradot Coulomb interaction, $U \equiv e^2/2C$ is the charging energy of QD.

By using the equation of motion, the retarded Green function of QD can be solved exactly. For example, for a three-level QD, $H_{dot} = \sum_{i=1}^3 E_i c_i^\dagger c_i + U(n_1 n_2 + n_2 n_3 + n_3 n_1)$, one obtains

$$\begin{aligned} \langle \langle c_1 | c_1^\dagger \rangle \rangle^r &= \frac{\langle (1-n_2)(1-n_3) \rangle}{\omega - E_1} + \frac{\langle (1-n_2)n_3 \rangle}{\omega - E_1 - U} \\ &+ \frac{\langle n_2(1-n_3) \rangle}{\omega - E_1 - U} + \frac{\langle n_2 n_3 \rangle}{\omega - E_1 - 2U} \end{aligned} \quad (\text{A2})$$

(ω contains an infinitesimal imaginary part $i0^+$, for all the retarded Green functions). The atomic-limit solution have clear physics meaning: due to intradot interaction, the single-particle energy level E_i exhibits several subresonances, $E_i, E_i + U, E_i + 2U, \dots$, the weights of these subresonances are determined by the occupation configuration of other energy levels. For the three-level QD, E_1 has the weight of $\langle (1-n_2)(1-n_3) \rangle$, i.e., the probability of both E_2 and E_3 are empty; $E_1 + U$ has the weights of $\langle (1-n_2)n_3 \rangle$ and $\langle n_2(1-n_3) \rangle$, i.e., the probability of one of E_2 and E_3 is occupied and the other empty; $E_1 + 2U$ has the weight of $\langle n_2 n_3 \rangle$, i.e., the probability of both E_2 and E_3 are occupied.

The calculation of the correlation functions like $\langle n_1 n_2 \rangle$ should be done self-consistently when QD is in the nonequilibrium distribution. However, for the equilibrium QD in the atomic limit, the calculation is straightforward. In this case, the thermal equilibrium QD can be depicted by the density

operator $\rho = (1/Z)e^{-\beta H_{dot}}$, and the observable $\langle O \rangle$ can be calculated by $\text{Tr}(\rho O)$. For the three-level QD, the results are listed in Table II, and the weights in Eq.(A2) can be evaluated with the help of this table, for example, $\langle n_2 n_3 \rangle = \langle (1-n_1)n_2 n_3 \rangle + \langle n_1 n_2 n_3 \rangle$.

Generally, QD with L energy levels may have 2^L occupation configurations, represented by $F = (N_1, N_2, \dots, N_L)$ with $N_i = 0$ or 1. One has

$$P(F) \equiv \left\langle \prod_{i=1}^L m_i \right\rangle = \frac{1}{Z} e^{-\beta E_{dot}(F)}, \quad (\text{A3})$$

$$m_i \equiv \begin{cases} n_i & \text{for } N_i = 1 \\ (1-n_i) & \text{for } N_i = 0, \end{cases}$$

in which $E_{dot}(F) \equiv \sum_i E_i N_i + U \sum_{i<j} N_i N_j$ is the total energy of QD for the configuration F . Define $\tilde{g}^r \equiv \sum_{i=1}^L \langle \langle c_i | c_i^\dagger \rangle \rangle^r$, it is easy to obtain

$$\tilde{g}^r = \sum_F P(F) g^r(F), \quad (\text{A4})$$

$$g^r(F) = \sum_{i=1}^L \frac{1}{\omega - \tilde{E}_i(F)},$$

in which $\tilde{E}_i(F) \equiv E_i + U \sum_{j \neq i} N_j$ is the renormalized single-particle level.

In short, in the atomic limit, the retarded Green function \tilde{g}^r is the average over different occupation configurations weighted by a thermal factor, and each configuration behaves as a set of renormalized single-particle levels.

*Author to whom correspondence should be addressed.

¹A. F. Andreev, Zh. Éksp. Teor. Fiz. **46**, 1823 (1964) [Sov. Phys. JETP **19**, 1228 (1964)].

²G. E. Blonder, M. Tinkham, and T. M. Klapwijk, Phys. Rev. B **25**, 4515 (1982).

³C. J. Lambert and R. Raimondi, J. Phys.: Condens. Matter **10**, 901 (1998).

⁴C. W. J. Beenakker, Phys. Rev. B **46**, 12 841 (1992).

⁵N. R. Clauphton, M. Leadbeater, and C. J. Lambert, J. Phys.: Condens. Matter **7**, 8757 (1995).

⁶Q.-f. Sun, J. Wang, and T.-h. Lin, Phys. Rev. B **59**, 3831 (1999).

⁷A. Golub, Phys. Rev. B **54**, 3640 (1996).

⁸R. Fazio and R. Raimondi, Phys. Rev. Lett. **80**, 2913 (1998).

⁹K. Kang, Phys. Rev. B **58**, 9641 (1998).

¹⁰P. Schwab and R. Raimondi, Phys. Rev. B **59**, 1637 (1999).

¹¹A. A. Clerk and V. Ambegaokar, Phys. Rev. B **61**, 3555 (2000).

¹²A.-P. Jauho, N. S. Wingreen, and Y. Meir, Phys. Rev. B **50**, 5528 (1994).

¹³A. L. Yeyati, F. Flores, and A. Martín-Rodero, Phys. Rev. Lett. **83**, 600 (1999).

¹⁴M. A. Kastner, Rev. Mod. Phys. **64**, 849 (1992).

¹⁵Y. Meir, N. S. Wingreen, and P. A. Lee, Phys. Rev. Lett. **66**, 3048 (1991).

¹⁶D. C. Ralph, C. T. Black, and M. Tinkham, Phys. Rev. Lett. **78**, 4087 (1997).

¹⁷S. Guéron *et al.*, Phys. Rev. Lett. **83**, 4148 (1999).

¹⁸A. L. Yeyati *et al.*, Phys. Rev. B **55**, R6137 (1997).

¹⁹H. Takayanagi and T. Akazaki, Phys. Rev. B **52**, R8633 (1995).

²⁰S. G. den Hartog *et al.*, Phys. Rev. Lett. **77**, 4954 (1996).

²¹P. H. C. Magnée *et al.*, Phys. Rev. B **50**, 4594 (1994).

²²Y. Dagan *et al.*, Phys. Rev. B **61**, 7012 (2000).